# Age matters: Fate of soil organic matter during ageing of earthworm casts produced by the anecic earthworm Amynthas khami

N. Bottinelli, M. Kaupenjohann, M. Märten, P. Jouquet, L. Soucémarianadin, François Baudin, T.M. Tran, C. Rumpel

# Age matters: fate of soil organic matter during ageing of earthworm casts produced by the anecic earthworm *Amynthas khami*

N. Bottinelli[1,2]; M. Kaupenjohann[3]; M. Märten[3]; P. Jouquet[1]; L. Soucémarianadin[4]; F. Baudin[5] ; T.T. Minh[2], C. Rumpel[1]

[1]CNRS, IRD, Institut d'écologie et des sciences de l'environnement (IESS Paris), Bondy, France

[2]Department of Soil sciences, Soils and Fertilizers Research Institute (SFRI), Hanoi, Vietnam

[3] Institute of Ecology, Department of Soil Science, Technische Universität, Berlin, Germany

[4]Laboratoire de Géologie, PSL Research University, CNRS-ENS UMR8538, Paris, France

[5] Sorbonne Université/CNRS, UMR ISTeP, 4 place Jussieu, Paris, France

Corresponding author: Nicolas Bottinelli

E-mail: nicolas.bottinelli@ird.fr

**Abstract**

The fate of organic matter (OM) occluded in earthworm casts during the casts' lifetime is poorly known. We collected casts produced by the anecic earthworm *Amynthas khami* in tropical woodland in Northern Vietnam at different times after their production. The aim of this study was to assess the (1) the effect of earthworms on biogeochemical OM properties compared to control aggregates, separated from the surrounding soil and (2) the fate of OM during cast ageing. We analysed five cast ageing stages for elemental content, OM chemical composition by analytical pyrolysis and stability by Rock-Eval thermal analysis. Moreover, we assessed the distribution of organic carbon (OC) in density fractions.

Compared to control aggregates, fresh casts had higher OC values (5.3 vs. 2.6 %) and increased OC in all density fractions. Cast OM had more lignin (1.1 *vs.* <0.1 %), similar polysaccharide and N-compound contribution and was more thermally labile than those of control aggregates. Changes in OM composition and content during cast ageing appeared at the end of the casts' lifetime, when they were broken into small sized aggregates (10-13 mm). At these latest stages, OC content decreased (1.5-fold); along with OM in macro-aggregates (2.2-fold) and microaggregates (6.8-fold). Reduced mineral-associated OC was also recorded (1.3-fold). During ageing, the percentage of lignin decreased (5.5-fold) while the thermal stability of OM increased. Most properties were still significantly different between the oldest ageing stage and control aggregates. This study highlights that the impact of earthworms on OM storage goes beyond cast disintegration and that there is a need to better understand their influence on soil organic matter stabilisation processes and in particular the formation and stability of organo-mineral associations.

**Key words:** soil, organic matter; aggregation; bioturbation; anecic earthworm cast

## 1. Introduction

Earthworms play an important role in the functioning of the soil system due to their bioturbation activity and the production of casts with specific physical, chemical and biological properties (Bottinelli et al., 2015; Van Groenigen et al., 2019). For example, fresh earthworm casts are known as biogeochemical hotspots (Kuzyakov and Blagodatskaya, 2015) and can be enriched in organic carbon (OC) and other nutrients (Van Groenigen et al., 2019) as compared to the surrounding topsoil. In the first hours after cast formation, plant-available nutrients may be released (Barois and Lavelle, 1986), because casts contain a high proportion of fresh organic matter (OM) (Guggenberger et al., 1996), which may be partly degraded shortly after their incorporation into macro-aggregates. Conversely, the formation of microaggregates (Bossuyt et al., 2005, 2004) and the association of OM to the mineral phase (Vidal et al., 2019) within the earthworm gut and/or within macro-aggregates might hamper OM mineralization in casts. During degradation of casts, the occluded OM (1) may become available again for microbial decay and mineralization processes when present in form of labile particulate organic matter (POM) or (2) may continue to contribute to OM storage if strongly associated to the mineral phase and/or included into stable microaggregates. There is little information about the time horizon of this protection in the field, where casts can disintegrate through physical disturbance, e.g. rainfall events. The very limited number of studies carried out under field conditions showed contradictory results, with an increase (Decaëns et al., 1999) or a decrease (McInerney et al., 2001) of OC in casts during ageing. Moreover, to the best of our knowledge, the effect of cast ageing on SOM composition and stability has rarely been assessed.

In North Vietnam, the anecic earthworm *Amynthas khami* (Megascolecidae family) produces large casts on the soil surface. These casts are enriched in OC, lignin and polysaccharides and reasonably water stable after their formation (Hong et al., 2011; Jouquet et al., 2008). During our extensive field work, we noticed that they may last for months to years. Thanks to their stability, casts from *A. khami* casts constitute therefore an interesting model for understanding changes in OC content and OM properties during cast ageing. Even if *A. khami* casts are rather stable after field deposition, we hypothesized that the processes affecting occluded OM during the casts' lifetime are similar to those affecting casts produced by other species. This study aimed to evaluate the biogeochemical changes occurring during the casts' lifetime. We collected surface earthworm casts of *A. khami* representing different stages of ageing in the field and investigated their biogeochemical cast properties and the distribution of OM in four different functional OM pools and compared them to adjacent control aggregates without visible earthworm influence. We hypothesized that (1) earthworm casts disintegrate after their formation due to disturbance events, (2) occluded OM changes during this process and (3) OM characteristics become similar to adjacent control aggregates at later ageing stages. Our specific objectives were to investigate (1) the effect of earthworms on biogeochemical OM properties, and (2) the fate of OM during cast ageing.

## 2. Materials and methods

### *2.1. Study site*

Soil and earthworm casts were sampled at the M-Tropics long-term observatory catchment located in the Dong Cao village in Northern Vietnam (20° 57'N, 105° 29'E). The climate in the region is subtropical humid with annual mean temperature of 20 °C and 1800 mm of rainfall. The dominant soil type is Acrisol (WRB)

(Podwojewski et al., 2008), characterized by an OC content of 2.5%, a clay content of 50% and a $pH_{KCl}$ of 3.9. Woodlands, secondary forests, meadows and fallows are the main land uses in the catchment. Surface earthworm activity in the catchment is high with the anecic earthworm *Amynthas khami* being the main species depositing casts on the soil surface. Samples were collected during the dry season in March 2017, in woodland, where the quantity of casts deposited at the soil surface was on average 4400 g (oven dry weight) $m^{-2}$.

*2.2. Soil sampling and preparation*

Soil in woodland is covered by recent and old earthworm casts that form a typical granular layer up to 5 cm thick. We compared casts of five contrasting stages of ageing and adjacent control aggregates without visible earthworm activity (ctrl). Sampling took place at five random locations in an area of 2500 $m^2$. We sampled five types of casts with contrasting stage of ageing differentiated by their humidity and degradation features (Fig. 1). The aging stages comprising five different cast types had been determined through detailed field observations: (1) cast-A: fresh casts, known to be < 1 day; (2) cast-B: fresh casts < 1 week old; (3) cast-C: dry casts, probably more than 1 month old; (4) cast-D: dry casts with marked signs of degradation (greenish colour due to the presence algae with cracks at the surface), older than cast-C. The size of casts (A to D) varied from 5 to 15 cm. They were produced through the accumulation of faecal pellets deposited the one on the other. After disintegration probably due to livestock trampling, human traffic, root growth and raindrop impact or natural aggregate turnover, individual pellet of 1 cm diameter are released: (5) cast-E of unknown age, consisting of small aggregates and representing the last stage of degradation recognizable by naked eyes. Differentiation

of old casts and soil aggregates is an unresolved problem faced by many workers in environments with high earthworm activity. In the present work, based on extensive field observations, we considered that control aggregates had no round shape and could in contrast to casts-E not be identified as earthworm casts by naked eyes. To sample control aggregates, we collected soil aggregates (5-15 cm) from 2-7 cm depth in the vicinity of the casts without visible earthworm influence.

The exact cast age was not very important for our study. We aimed at describing the biogeochemical OM changes occurring during ageing, and therefore sampled an age gradient of casts based on morphological cast properties determined through extensive fieldwork. During ageing, these stages follow one another, at varying timescales depending on the actual lifetime of the cast, which is depending on climatic conditions and the occurrence of disturbance events.

In total, 30 samples were collected: (5 types of casts + 1 control) × 5 replicates. To work on samples with similar physical properties, we air-dried and broke up manually the earthworm casts and ctrl samples into aggregates between 10 and 13 mm.

*2.3. Physical fractionation of and isolation of particulate organic matter (POM)*

Before starting fractionation, the samples were hydrated for 2 h. Thereafter, they were automatically shaken in water and wet-sieved at 2 mm for 3 h at 140 rotations per minute. The material < 2mm was filtered and the soil remaining on the filter paper was air-dried for two days. The dry material < 2mm was subjected to density fractionation using SPT (Na–polytungstate) with a density of 1.67 $g \cdot cm^{-3}$ following the method suggested by Cerli et al. (2012). We isolated four density fractions: free

151 particulate organic matter (fPOM), two occluded particular organic matter fractions
152 (oPOM) and the remaining heavy fraction (HF). Briefly, 10 g of sieved soil or casts
153 were mixed with 67.2 ml Na–polytungstate solution with a density of 1.67 $g \cdot cm^{-3}$ and
154 the fPOM fraction was recovered by filtration after gently shaking and centrifuging
155 (3,500 rpm for 30 min). The fraction was washed with distilled water and freeze-
156 dried. The remaining soil in the polytungstate solution was treated with
157 ultrasonication (40 J $ml^{-1}$) to disperse macro-aggregates and release the occluded
158 particulate organic matter (oPOM) fraction. After recovery of this fraction by
159 centrifugation and filtration, the procedure was repeated with stronger ultrasonication
160 (400 J $ml^{-1}$) to completely disperse the samples and to recover POM occluded in
161 micro-aggregates. The remaining material represented mineral-associated OC of the
162 heavy fraction. All fractions were freeze-dried, weighted, crushed at 200µm and
163 analyzed for OC and N content. To determine the contribution of the four OM pools
164 isolated by density fractionation to the total SOC content, we calculated the mass of
165 OC present in the fractions. We considered that fPOM and oPOM (40 $J \cdot ml^{-1}$)
166 indicated POM stored in macro-aggregates whereas oPOM (400 $J \cdot ml^{-1}$) indicated
167 POM stored in micro-aggregates. HF represented the OM associated to the mineral
168 phase. Total OC and N of bulk samples and physical fractions were measured using
169 an elemental analyser (Thermo Flash HT, Thermo Fisher Scientific Inc., Waltham,
170 USA). The mean OC recovery after the density fractionation procedure was 92%.
171
172 2.4. *Molecular composition of SOM: analytical pyrolysis*
173 Bulk samples were subjected to analytical pyrolysis to investigate the molecular
174 composition of their OM. The analyses were carried out with a pyrolysis unit (GSG
175 Curie point Pyrolyser 1040 PSC) coupled to a gas chromatograph (Hewlett Packard

176 HP 5890) and a mass spectrometer (Hewlett Packard HP 5889; electron energy 70
177 eV). Briefly, 0.5–1 mg of sample were loaded in tubular ferromagnetic wires,
178 inductively heated to their Curiepoint temperature of 650 °C in 0.15 sec in the
179 pyrolysis unit. The pyrolysis products were transferred to the GC system operating in
180 spitless mode with He as carrier gas (flow 1 ml/min). They were separated on a 60 m
181 fused silica capillary column with a wax stationary phase (SolGelWax, SGE, 0.32 mm
182 i.d., film thickness 0.5 µm) before being detected using quadrupole mass
183 spectrometry. The temperature of the GC oven was programmed from 30 °C to
184 280 °C at 2 °C/min. The final temperature was hold for 15 min. Pyrolysis releases a
185 suite of pyrolysis products. We chose a polar column, because we were interested in
186 the relative quantification of polysaccharide-derived, lignin-derived and N-containing
187 pyrolysis products as main SOM compounds from the GC traces. Such compounds
188 were found to yield broad peaks when separated on a non-polar column (Dignac et al.,
189 2006). We quantified the relative contribution of these compounds after their
190 identification using the total ion chromatogram.
191
192 *2.5. Thermal analysis: Rock-Eval 6*
193 We used a Rock-Eval 6 turbo device (Behar et al., 2001) for the thermal analysis of
194 bulk samples. We adapted the procedure developed for the analysis of SOM proposed
195 by Disnar et al. (2003) as specified in Soucémarianadin et al. (2018). Briefly, about 60
196 mg of ground sample were subjected to two consecutive thermal treatments: first,
197 samples were transferred to a pyrolysis oven (under $N_2$ atmosphere) then to a
198 combustion oven (under laboratory air atmosphere). Effluents released during the
199 pyrolysis contained mostly hydrocarbons or HC. They were detected and quantified
200 by a flame ionization detector; during both the pyrolysis and oxidation stages. CO and

$CO_2$ were detected with an infrared detector. We determined two standard parameters: the hydrogen index (HI) and the oxygen index ($OI_{RE6}$). HI is defined as the amount of pyrolyzed HC relative to the total OC content of the sample and shows the relative enrichment (high HI) or depletion (low HI) of OC in hydrogen-rich moieties. $OI_{RE6}$ is defined as the amount of oxygen present as CO and $CO_2$ during the pyrolysis stage divided by the total OC content of the sample (Lafargue et al., 1998). The $OI_{RE6}$ describes the relative oxidation status of OC. Other indexes proposed by Sebag et al. (2016) were calculated by integrating the pyrolysis curve between predefined temperature thresholds to describe the OM thermal stability. The R-index, which ranges from 0 to 1, corresponds to the relative contribution of thermally stable OM with refractory compounds released at higher temperature. The I-index provides information on the preservation of thermally labile immature OM, with compounds released at lower temperatures (Sebag et al., 2016). We also calculated $T_{50\_CO2\_PYR}$ and $T_{50\_CO2\_OX}$ (Cécillon et al., 2018), which are the temperature at which 50% of the $CO_2$ are released during pyrolysis and combustion.

2.6. *Statistical analysis*

One-way ANOVAs were used to test the effect of earthworm activity on soil properties. We compared casts of different degradation stages and ctrl samples (n = 5). Prior to running ANOVAs, data were tested for homogeneity of variances and normality and log-transformed when required. LSD post hoc multiple comparison tests were used if the effects were significant. Differences among treatments were declared significant at the 0.05 probability level. We also performed between-class analyses (BCA) and Monte Carlo permutation tests (1000 permutations) to exploit the information of the (i) pyrolysis compounds, (ii) Rock-Eval 6 thermal stability

parameters and (iii) all properties characterizing OM in casts. All statistical calculations and plots were executed with R 3.12 statistical package for Windows (http://www.r-project.org) using "car", "ade4" and "ggplot2" packages.

## 3. Results

### *3.1. OC content of bulk samples and density fractions*

The OC content of cast-A was twice as high as those of ctrl samples, and gradually decreased during cast ageing (**Table 1**). All cast types showed a significantly higher OC content than samples from ctrl samples, while their C/N ratios were similar (**Table 1**).

The OC allocation to specific pools changed between casts and ctrl samples (**Table 1**). In all samples, the vast majority of OC, representing between 83 and 94% was found in the mineral-associated fraction. Between 5 and 12% of OC was occluded in macro-aggregates and up to 5% of OC was present in micro-aggregates.

It was interesting to note that earthworm activity increased the total amount of OC in the mineral-associated fraction of fresh casts (cast-A versus ctrl), but that this OC was also decreasing during cast ageing (from cast-A to cast-E). We observed that total OC storage decreased from casts-A to -E by 69% in the microaggregate fraction, by 50% in the macro-aggregate fraction and by 29% in the mineral-associated fraction. Despite this decrease, the latter fraction was the only one, which showed significantly higher OC amounts in cast-E as compared to ctrl samples. Overall, the C/N ratio was lowest in the mineral-associated fraction, highest in micro-aggregates and intermediate in macro-aggregates (**Table 1**). Cast-A showed higher C/N ratio than ctrl samples, for macro-aggregate and mineral-associated OM, lower C/N ratios in macro-aggregates and slightly lower C/N ratios in the mineral-associated fraction as

compared to ctrl aggregates. From cast-A to -E, the C/N ratio was quite stable and significantly different than for ctrl aggregates.

*3.2. Molecular composition of bulk samples*

Pyrolysis products showing significant differences among samples and their possible origin are shown in **Table 2**. All pyrograms were characterised by contribution of N-containing products, which represented between 30 and 34% of the Total Iron Chromatogram (TIC). Polysaccharide-derived pyrolysis products contributed between 13 and 17% to the TIC, and most compounds did not show any significant differences among cast ageing stages and/or ctrl. Furfural was the only compound, which showed a higher contribution in casts than ctrl (**Table 2**). The most significant peaks, representing 50 to 60% to the TIC were attributed to compounds of unspecific origin. Lignin-derived compounds contributed less than 1–2% to the TIC and were identified in cast samples only (**Table 2**).

Cast-A was characterized by higher percentage of lignin, lower percentage of unspecific compounds and similar percentages of polysaccharides and N-containing compounds in comparison to ctrl aggregates. The percentage of lignin decreased from cast-A to cast-E, which showed similar values than ctrl aggregates. The percentage of unspecific compounds was stable from cast-A to cast-E and significantly different to ctrl aggregates (**Table 2**). The BCA of pyrolysis products showed that the cast ageing stages were differentiated into three groups: (1) cast-A to cast-D, (2) cast-E and (3) ctrl on the first and second axis, which explained 91% of the total variability. Cast-A was characterized by higher contribution of P5, U9, U6, L1, N10 and lower contribution of U1, U7 and N2 than ctrl samples. From cast-A to cast-E, the

276 percentage of P5 decreased. Cast-E samples were significantly different from ctrl for
277 all the properties except for P5 and N8.
278
279 3.3. *Thermal stability of OM in bulk samples*
280 All variables were significantly influenced by the presence of earthworms and ageing
281 of casts (**Table 3**). The HI, $OI_{RE6}$ and $T_{50\_CO2\_OX}$ were more sensitive than I-index, R-
282 index and $T_{50\_CO2\_PYR}$ according to the F-values. BCA of the thermal stability
283 parameters (**Fig. 3**) separated samples into 3 groups: (1) cast-A to -D, (2) cast-E and
284 (3) ctrl aggregates on the first and second axis, which explained 93% of the total
285 variability. Cast-A was characterized by higher values of HI, and lower values of
286 $OI_{RE6}$, R-index, $T_{50\_CO2\_PYR}$ and $T_{50\_CO2\_OX}$ than ctrl samples. Conversely, the I-index
287 was similar in cast-A and ctrl aggregates. From cast-A to cast-E, HI and I-indexes
288 decreased whereas $OI_{RE6}$, the R-index and $T_{50\_CO2\_OX}$ increased. In cast-E samples,
289 HI, $OI_{RE6}$, I-index and $T_{50\_CO2\_OX}$ were still significantly different from ctrl
290 aggregates.
291
292 **4. Discussion**
293 *4.1. Earthworm-induced changes in OM properties during cast formation*
294 *4.1.1 Quantitative changes of organic matter pools*
295 The OC content of cast-A doubled as compared to ctrl aggregates, which is in
296 agreement with many other studies concerning the influence of earthworms on soil
297 properties (reviewed by Van Groenigen et al., 2019). Our results indicated that this
298 was due to greater amounts of OC associated to the mineral fraction, which increased
299 by 50% through earthworm activity. A high proportion of mineral-associated OC in
300 earthworm casts is in agreement with results of Vidal et al. (2019), who showed that

90% of the OC in casts was associated to the mineral fraction. The presence of a high amount of this material in cast-A could indicate that organo-mineral associations were formed within the earthworm gut (LeMer et al., 2020). Although such a process has been hypothesised for long (Shipitalo and Protz, 1989), to the best of our knowledge this study is among the first to provide quantitative evidence of organo-mineral formation through earthworm activity under field conditions. The amount of OC in macro- and micro-aggregates contributed together for only 16% of the total OC. OM protection by occlusion in macro- and micro-aggregates is a well-known phenomenon and is generally assumed to be the most important process stabilizing OM following earthworm activity (Bossuyt et al., 2004, 2005). Our data indicate, that physico-chemical protection of OM in earthworm casts may at least be equally important. A recent laboratory study showed that such protection may affect completely degraded as well as fresh OM compounds (Barthod et al., 2020).

*4.1.2 Qualitative changes of OM during cast ageing*

Cast-A had higher percentages of lignin than ctrl aggregates showing that anecic species like *A. Khami* ingest a mixture of soil and fresh plant debris (Guggenberger et al., 1996; Hong et al., 2011). This is also supported by the molecular composition, which indicated the higher contribution of furfural, a polysaccharide compound, in cast-A than ctrl aggregates. The rather undecomposed nature of OM in cast-A is supported by the Rock-Eval 6 thermal stability parameters. Cast-A had a higher HI and I-index and lower $OI_{RE6}$, R-index, $T_{50\_CO2\_OX}$ and $T_{50\_CO2\_PYR}$ than ctrl aggregates. Theses parameters are all indicative of fresh, easy decomposable OM compounds with a low thermal stability (Cécillon et al., 2018; Schomburg et al., 2018; Sebag et al., 2016; Soucémarianadin et al., 2019). Our result is in agreement with a study

showing that OM in casts formed by an anecic *Martiodrilus* species is more labile than in ctrl aggregates (Guggenberger et al., 1996). Conversely, Schomburg et al. (2018) showed in experimental conditions that the belowground casting activity of the endogeic species *Allolobophora chlorotica* lead to the decrease in decomposable OM compounds and to the increase of its thermal stability in soil aggregates. These contradictory results are most probably related to the different feeding activity of anecic and endogeic species.

*4.2. Changes in OM storage and quality during cast ageing in the field*

The OC content of casts remained similar from cast-A to -C and decreased thereafter. In contrast, the molecular composition of cast changes in the first ageing stages. From cast-A to -C the contribution of lignin and N-containing compounds increased (significant for L1 and N10). It is likely that the lower porosity of casts as compared to ctrl samples (Bottinelli et al., 2012) prevented the mineralization of OM and thus led to transformation of OM compounds. A similar explanation was suggested by Martin (1991), who found no change of OC content in casts during a laboratory incubation of 420 days. Changes in chemical composition were similar to those observed upon microbial decomposition of crop residues in soil (Franchini et al., 2002) and may reflect microbial use of easily decomposable polysaccharides leading to selective preservation of lignin and simultaneously accumulation of N-containing compounds of microbial origin (Kögel-Knabner and Rumpel, 2018). The chemical changes in the first three cast ageing stages may thus be related to an intense activity of micro-organisms occurring in earthworm casts (Aira et al., 2005; Tiunov and Scheu, 2000).

Most significant changes appeared in later cast ageing stages, and in particular when casts were broken into small-sized aggregates (cast-E). Changes from casts-A to -E included gradual OC loss from all physical fractions, representing a total loss of 32% of OC. Similar observations were made by McInerney et al. (2001), who studied ageing of surface casts produced by the epi-anecic *L. terrestris* and found that OM decreased by 15% 2.5 years after field exposure. Our results are however in contrast to a study by Decaëns et al. (1999), who found a doubling of the OC content in casts produced by the anecic *M. carimaguensis* after 330 days. These contrasting results may indicate that OC dynamics in casts may be influenced differently by different earthworm species and possibly also by their environment (i.e., climate, vegetation and soil properties). Our results indicated that OC associated to micro-aggregates was lost after cast disintegration along with a high proportion of presumably stable OC associated to the mineral fraction. This could be related to enhanced decomposition after exposure to microbial activity but may also be due to loss of small particles following rainfall events (Barthes and Roose, 2002). Although presumably stable OC associated with the mineral fraction was lost during ageing, the bulk OC was characterized by a higher thermal stability and less labile plant material after ageing (cast-A to -E) and higher contribution of N-containing and unspecific compounds, which generally accumulates during degradation and stabilization processes of OM in soils (Kögel-Knabner and Rumpel, 2018).

To summarize the impact of earthworms on OM properties, we performed a between-class analysis (BCA) (**Fig. 4**). Our analysis indicated that OM properties were changing when casts were broken into small aggregates (10-13 mm) (cast-E). The latest ageing stage, however, kept specific properties significantly different from ctrl

samples, and was not on the trajectory towards ctrl aggregates on the BCA plan. As we hypothesized that eventually cast properties should become similar to those of ctrl aggregates, further studies are needed to investigate the timescale at which this happens and what processes are involved. Such information is important in the studied ecosystem because of the large quantity of soil and OC excreted by *A. Khami* as casts. Based on a soil bulk density of 1.0 $g \cdot cm^{-3}$, the total quantity of OC in casts represented 6 to 9% of the topsoil (10 cm depth) depending if casts were degraded (cast-E) or recent (cast-A). We therefore suggest that the processes leading to their ageing are important in terms of SOC dynamics, through changing SOC chemical composition and its distribution in stabilized SOM pools.

## Conclusions

In this study we investigated the fate of SOM during cast ageing. The anecic behaviour of the earthworm *A. khami* leads to the incorporation of fresh OM in their casts. In addition, increased occlusion of OM in micro-aggregates and higher amounts of OM associated to mineral surfaces in casts as compared to ctrl suggested a high potential for OC storage. Our results indicated gradual changes in OM chemical composition and increased thermal stability during ageing. In addition, ageing led to disintegration of aggregates and the decrease of OM in all physical fractions. Even OM associated to the mineral phase containing presumably large amounts of stable OC showed strong dynamics. Our results thus suggest that earthworm activity accelerates SOM dynamics in stabilized pools. Since casts presenting the ultimate degradation stage recognized by the naked eye kept specific OM properties different from the ctrl aggregates, more studies are needed to understand the time horizons and ecological mechanisms affecting SOC transformation in the last cast ageing stages.

**Acknowledgments**

This project was financially supported by CNRS/INSU (VINAWORM) research program under the framework of the EC2CO program. We acknowledge the technical assistance of the farmers in Dong Cao village.

**References**

Aira, M., Monroy, F., Domínguez, J., 2005. Ageing effects on nitrogen dynamics and enzyme activities in casts of Aporrectodea caliginosa (Lumbricidae). Pedobiologia 49, 467–473. doi:10.1016/j.pedobi.2005.07.003

Barois, I., Lavelle, P., 1986. Changes in respiration rate and some physicochemical properties of a tropical soil during transit through Pontoscolex corethrurus (glossoscolecidae, oligochaeta). Soil Biology and Biochemistry 18, 539–541. doi:10.1016/0038-0717(86)90012-X

Barthès, B. and Roose, E., 2002. Aggregate stability as an indicator of soil susceptibility to runoff and erosion : validation at several levels. Catena, 47, 133-149. doi: 10.1016/S0341-8162(01)00180-1

Barthod, J., Dignac, M.-F., Mer, G. Le, Bottinelli, N., Watteau, F., Kögel-Knabner, I., Rumpel, C., 2020. How do earthworms affect organic matter decomposition in the presence of clay-sized minerals? Soil Biology and Biochemistry 107730. doi:https://doi.org/10.1016/j.soilbio.2020.107730

Behar, F., Beaumont, V., De B. Penteado, H.L., 2001. Rock-Eval 6 Technology: Performances and Developments. Oil & Gas Science and Technology 56, 111–134. doi:10.2516/ogst:2001013

Bossuyt, H., Denef, K., Six, J., Frey, S.D., Merckx, R., Paustian, K., 2001. Influence of microbial populations and residue quality on aggregate stability. Applied Soil

426 Ecology 16, 195–208. doi:10.1016/S0929-1393(00)00116-5
427 Bossuyt, H., Six, J., Hendrix, P.F., 2005. Protection of soil carbon by microaggregates
428 within earthworm casts. Soil Biology and Biochemistry 37, 251–258.
429 doi:10.1016/j.soilbio.2004.07.035
430 Bossuyt, H., Six, J., Hendrix, P.F., 2004. Rapid incorporation of carbon from fresh
431 residues into newly formed stable microaggregates within earthworm casts.
432 European Journal of Soil Science 55, 393–399. doi:10.1111/j.1351-
433 0754.2004.00603.x
434 Bottinelli, N., Jouquet, P., Capowiez, Y., Podwojewski, P., Grimaldi, M., Peng, X.,
435 2015. Why is the influence of soil macrofauna on soil structure only considered
436 by soil ecologists? Soil and Tillage Research 146, 118–124.
437 doi:10.1016/j.still.2014.01.007
438 Bottinelli, N., Jouquet, P., Tran, T.D., Hallaire, V., 2012. Morphological
439 characterisation of weathered earthworm casts by 2D-image analysis. Biology
440 and Fertility of Soils 48, 845–849. doi:10.1007/s00374-012-0674-5
441 Cécillon, L., Baudin, F., Chenu, C., Houot, S., Jolivet, R., Kätterer, T., Lutfalla, S.,
442 Macdonald, A., Van Oort, F., Plante, A.F., Savignac, F., Soucémarianadin, L.N.,
443 Barré, P., 2018. A model based on Rock-Eval thermal analysis to quantify the
444 size of the centennially persistent organic carbon pool in temperate soils.
445 Biogeosciences 15, 2835–2849. doi:10.5194/bg-15-2835-2018
446 Cerli, C., Celi, L., Kalbitz, K., Guggenberger, G., Kaiser, K., 2012. Separation of light
447 and heavy organic matter fractions in soil - Testing for proper density cut-off and
448 dispersion level. Geoderma 170, 403–416. doi:10.1016/j.geoderma.2011.10.009
449 Decaëns, T., Rangel, A.F., Asakawa, N., Thomas, R.J., 1999. Carbon and nitrogen
450 dynamics in ageing earthworm casts in grasslands of the eastern plains of

Colombia. Biology and Fertility of Soils 30, 20–28. doi:10.1007/s003740050582

Dignac, M.F., Houot, S., Derenne, S., 2006. How the polarity of the separation column may influence the characterization of compost organic matter by pyrolysis-GC/MS. Journal of Analytical and Applied Pyrolysis 75, 128–139. doi:10.1016/j.jaap.2005.05.001

Disnar, J.R., Guillet, B., Keravis, D., Di-Giovanni, C., Sebag, D., 2003. Soil organic matter (SOM) characterization by Rock-Eval pyrolysis: Scope and limitations. Organic Geochemistry 34, 327–343. doi:10.1016/S0146-6380(02)00239-5

Franchini, J.C., Gonzalez-Vila, F.J., Rodriguez, J., 2002. Decomposition of plant residues used in no-tillage systems as revealed by flash pyrolysis. Journal of Analytical and Applied Pyrolysis 62, 35–43. doi:10.1016/S0165-2370(00)00210-2

Guggenberger, G., Thomas, R.J., Zech, W., 1996. Soil organic matter within earthworm casts of an anecic-endogeic tropical pasture community, Colombia. Applied Soil Ecology 3, 263–274. doi:10.1016/0929-1393(95)00081-X

Hong, H.N., Rumpel, C., Henry des Tureaux, T., Bardoux, G., Billou, D., Tran Duc, T., Jouquet, P., 2011. How do earthworms influence organic matter quantity and quality in tropical soils? Soil Biology and Biochemistry 43, 223–230. doi:10.1016/j.soilbio.2010.09.033

Jouquet, P., Podwojewski, P., Bottinelli, N., Mathieu, J., Ricoy, M., Orange, D., Tran, T.D., Valentin, C., 2008. Above-ground earthworm casts affect water runoff and soil erosion in Northern Vietnam. Catena 74, 13–21. doi:10.1016/j.catena.2007.12.006

Kögel-Knabner, I., Rumpel, C., 2018. Advances in Molecular Approaches for Understanding Soil Organic Matter Composition, Origin, and Turnover: A

476 Historical Overview. Advances in Agronomy 149, 1–48.
477 doi:10.1016/bs.agron.2018.01.003
478 Kuzyakov, Y., Blagodatskaya, E., 2015. Microbial hotspots and hot moments in soil:
479 Concept & review. Soil Biology and Biochemistry 83, 184–199.
480 doi:10.1016/j.soilbio.2015.01.025
481 McInerney, M., Little, D.J., Bolger, T., 2001. Effect of earthworm cast formation on
482 the stabilization of organic matter in fine soil fractions. European Journal of Soil
483 Biology 37, 251–254. doi:10.1016/S1164-5563(01)01092-5
484 Podwojewski, P., Orange, D., Jouquet, P., Valentin, C., Nguyen, V.T., Janeau, J.L.,
485 Tran, D.T., 2008. Land-use impacts on surface runoff and soil detachment within
486 agricultural sloping lands in Northern Vietnam. Catena 74, 109–118.
487 doi:10.1016/j.catena.2008.03.013
488 Schomburg, A., Verrecchia, E.P., Guenat, C., Brunner, P., Sebag, D., Le Bayon, R.C.,
489 2018. Rock-Eval pyrolysis discriminates soil macro-aggregates formed by plants
490 and earthworms. Soil Biology and Biochemistry 117, 117–124.
491 doi:10.1016/j.soilbio.2017.11.010
492 Sebag, D., Verrecchia, E.P., Cécillon, L., Adatte, T., Albrecht, R., Aubert, M.,
493 Bureau, F., Cailleau, G., Copard, Y., Decaens, T., Disnar, J.R., Hetényi, M.,
494 Nyilas, T., Trombino, L., 2016. Dynamics of soil organic matter based on new
495 Rock-Eval indices. Geoderma 284, 185–203.
496 doi:10.1016/j.geoderma.2016.08.025
497 Shipitalo, M.J., Protz, R., 1989. Chemistry and micromorphology of aggregation in
498 earthworm casts. Geoderma 45, 357–374. doi:10.1016/0016-7061(89)90016-5
499 Soucémarianadin, L., Cécillon, L., Chenu, C., Baudin, F., Nicolas, M., Girardin, C.,
500 Barré, P., 2018. Is Rock-Eval 6 thermal analysis a good indicator of soil organic

carbon lability? – A method-comparison study in forest soils. Soil Biology and Biochemistry 117, 108–116. doi:10.1016/j.soilbio.2017.10.025

Soucémarianadin, L., Cécillon, L., Chenu, C., Baudin, F., Nicolas, M., Girardin, C., Delahaie, A., Barré, P., 2019. Heterogeneity of the chemical composition and thermal stability of particulate organic matter in French forest soils. Geoderma 342, 65–74. doi:10.1016/j.geoderma.2019.02.008

Tiunov, A. V., Scheu, S., 2000. Microbial biomass, biovolume and respiration in Lumbricus terrestris L. cast material of different age. Soil Biology and Biochemistry 32, 265–275. doi:10.1016/S0038-0717(99)00165-0

Van Groenigen, J.W., Van Groenigen, K.J., Koopmans, G.F., Stokkermans, L., Vos, H.M.J., Lubbers, I.M., 2019. How fertile are earthworm casts? A meta-analysis. Geoderma 338, 525–535. doi:10.1016/j.geoderma.2018.11.001

Vidal, A., Watteau, F., Remusat, L., Mueller, C.W., Nguyen Tu, T.T., Buegger, F., Derenne, S., Quenea, K., 2019. Earthworm cast formation and development: A shift from plant litter to mineral associated organic matter. Frontiers in Environmental Science 7, 55. doi:10.3389/fenvs.2019.00055

526 **Figure caption**

527 **Figure 1:** Earthworm cast ageing stages. Cast-A: fresh casts, known to be < 1 day;
528 cast-B: fresh casts < 1 week old; cast-C: dry cast and probably more than 1 month old;
529 cast-D: dry cast with marked signs of degradation (greenish colour due to the
530 presence algae with cracks at the surface), older than cast-C; cast-E: casts broken in
531 small aggregates (10-13 mm) representing the last state of degradation recognizable
532 by naked eyes possibly more than 1 year old.

533

534 **Figure 2:** Biplot showing the between components analysis (BCA) from variables
535 describing the chemical composition OM for for the five cast ageing stages and for
536 control aggregates (Ctrl) presenting no recent earthworm activity. Only significant
537 compounds (Table 2) were included into the analysis. Variables are L1: 2-Methoxy-
538 phenol (guaiacol), N2: Pyridine, N8: Benzonitrile, N10: Benzenepropanenitrile, U1:
539 Benzene, U6: Acetic acid, U7: Naphtalene, U9: 4-Methyl-phenol/2- oder 3-Methyl-
540 phenol.

541

542 **Figure 3:** Biplot showing the between components analysis (BCA) from variables
543 describing the Rock-Eval 6 thermal stability parameters for the five cast ageing stages
544 and for control aggregates (Ctrl) presenting no recent earthworm activity. Variables
545 are HI for hydrogen index, $OI_{RE6}$ for oxygen index, R-index for refractory index, I-
546 index for immature index, $T_{50\_CO2\_PYR}$ corresponding to the temperature at which 50%
547 of the $CO_2$ resulting from organic matter pyrolysis had evolved and $T_{50\_CO2\_OX}$
548 corresponding to the temperature at which 50% of the $CO_2$ resulting from organic
549 matter oxidation had evolved.

**Figure 4:** Biplot showing the between components analysis (BCA) from variables describing OM for for the five cast ageing stages and for control aggregates (Ctrl) presenting no recent earthworm activity. Variables described the OM composition in purple (lignin, N-containing, polysaccharides and unspecific), the Rock-Eval 6 thermal stability parameters in blue (HI for hydrogen index, $OI_{RE6}$ for oxygen index, R-index for refractory index, I-index for immature index, $T_{50\_CO2\_PYR}$ corresponding to the temperature at which 50% of the $CO_2$ resulting from organic matter pyrolysis had evolved and $T_{50\_CO2\_OX}$ corresponding to the temperature at which 50% of the $CO_2$ resulting from organic matter oxidation had evolved), the OC content and C/N ratio of the whole aggregate and the three physical fractions (macroaggregate (macro), microaggregates (micro) and mineral-associated (min)).

**Table 1:** Average values and standard deviation (n=5) of OC content and C/N ratio of the bulk samples, and distribution of OC and the C/N ratio in the three physical fractions for the five cast ageing stages and for control aggregates (Ctrl) presenting no recent earthworm activity. Different letters indicate statistically significantly differences (*** $p < 0.001$; ** $p < 0.01$; * $p < 0.05$ and ns for $p > 0.05$).

| Properties | Ctrl | Cast-A | Cast-B | Cast-C | Cast-D | Cast-E | F and p-values |
|---|---|---|---|---|---|---|---|
| **Bulk aggregates** | | | | | | | |
| OC (mg $g^{-1}$) | 25.9 (4.2) d | 52.6 (6.6) a | 49.5 (4.1) ab | 54.4 (2.0) a | 44.8 (3.8) b | 35.9 (4.4) c | 31.2 *** |
| C/N | 12 (0.4) | 12.3 (0.5) | 12.7 (1.1) | 12.4 (0.8) | 12.1 (0.8) | 12.1 (0.4) | 1.4 ns |
| **Physical fractions** | | | | | | | |
| OC-macro-aggregates (% of bulk) | 5.9 (2.3) | 11.9 (4.4) | 9.8 (4.0) | 11.4 (5.0) | 8.6 (4.3) | 7.7 (2.5) | 1.5 ns |
| OC-micro-aggregates (% of bulk) | 0.0 (0.0) c | 4.5 (3.4) a | 4.9 (1.5) a | 4.7 (2.6) a | 2.8 (2.6) ab | 1.0 (1.3) bc | 6.1 *** |
| OC-mineral-associated (% of bulk) | 94.1 (2.3) a | 83.6 (7.7) bc | 85.2 (4.4) bc | 83.9 (6.9) c | 88.6 (5.4) abc | 91.3 (3.3) ab | 2.8 * |
| OC-macro-aggregates (mg) | 15.2 (5.5) c | 62.6 (29.8) a | 48.6 (19.5) ab | 61.8 (28.9) a | 38.4 (21.8) abc | 27.9 (9.2) bc | 5.9 ** |
| OC-micro-aggregates (mg) | 0.0 (0.0) b | 23.7 (2.1) a | 24.4 (6.8) a | 25.6 (14.2) a | 12.7 (11.9) ab | 3.5 (4.9) b | 6.5 *** |
| OC-mineral-associated (mg) | 244.4 (43.5) d | 439.8 (30.8) ab | 421.6 (48.3) ab | 456.7 (35.9) a | 396.9 (33.0) b | 328.8 (44.9) c | 22.2 *** |
| C/N-macro-aggregates | 23.9 (4.2) a | 16.4 (1.6) bc | 15.0 (2.2) c | 14.7 (2.5) c | 15.5 (1.5) c | 18.4 (1.6) b | 14.4 *** |
| C/N-micro-aggregates | - | 18.4 (6.5) | 17.5 (3.8) | 18.1 (7.2) | 18.4 (4.8) | - | 0.7 ns |
| C/N-mineral-associated | 8.9 (0.4) c | 9.7 (0.5) b | 9.6 (0.5) b | 10.2 (0.3) a | 9.6 (0.4) b | 9.6 (0.4) b | 5.7 ** |

Cast-A: fresh casts, known to be < 1 day; cast-B: fresh casts < 1 week old; cast-C: dry cast and probably more than 1 month old; cast-D: dry cast with marked signs of degradation (greenish colour due to the presence algae with cracks at the surface), older than cast-C; cast-E: casts broken in small aggregates (10-13 mm) representing the last state of degradation recognizable by naked eyes.

576 **Table 2:** Average values and standard deviation (n = 5) for the five cast ageing stages and for control aggregates (Ctrl) presenting no recent

577 earthworm activity. Different letters indicate statistically significant differences (*** p < 0.001; ** p < 0.01; * p < 0.05 and ns for p > 0.05).

| Origin | Code | Ctrl | Cast-A | Cast-B | Cast-C | Cast-D | Cast-E | F and p-values |
|---|---|---|---|---|---|---|---|---|
| Lignin (%) | L | 0.0 (0.0) d | 1.8 (0.5) b | 0.8 (0.1) c | 1.8 (0.6) a | 0.5 (0.1) c | 0.2 (0.3) d | 28.6 *** |
| 2-Methoxy-phenol | L1 | 0 (0.0) d | 0.4 (0.2) bc | 0.5 (0.1) b | 0.9 (0.3) a | 0.5 (0.1) b | 0.2 (0.3) cd | 11.8*** |
| N-containing (%) | N | 31.9 (3.1) | 33.4 (3.1) | 37.1 (5.4) | 33.6 (2.7) | 33.6 (1.9) | 38.6 (5.6) | 2.3 ns |
| Pyridine | N2 | 6.5 (1.8) a | 4.5 (0.4) bc | 4.5 (0.3) bc | 4.3 (0.7) c | 5.3 (0.4) b | 5.1 (1.2) bc | 6.9 *** |
| Benzonitrile | N8 | 4.8 (1.4) a | 4.8 (0.9) ab | 3.6 (0.3) abc | 2.6 (1.3) c | 4.0 (0.3) ab | 3.3 (1.5) bc | 3.1 * |
| Benzenepropanenitrile | N10 | 0.3 (0.2) b | 0.9 (0.2) b | 0.8 (0.1) b | 2.4 (2.3) a | 0.9 (0.1) b | 0.8 (0.1) b | 2.9 * |
| Polysaccharides (%) | P | 10.8 (3.4) | 14.5 (4.9) | 12.6 (0.9) | 16.6 (3.9) | 16.4 (3.0) | 13.5 (1.9) | 2.4 ns |
| Furfural | P5 | 1.5 (1.4) c | 3.4 (1.4) ab | 2.8 (0.5) abc | 2.4 (0.8) bc | 3.9 (1.2) a | 2.0 (0.2) bc | 3.4 * |
| Unspecific (%) | U | 57.2 (5.9) a | 50.3 (2.8) b | 49.6 (4.7) b | 45.4 (6.4) b | 49.5 (2.5) b | 47.7 (6.9) b | 2.9 * |
| Benzene | U1 | 17.1 (6.4) a | 8.8 (2.4) b | 7.8 (1.0) b | 5.5 (1.5) b | 8.1 (1.1) b | 8.1 (3.3) b | 8.1 *** |
| Acetic acid | U6 | 0.0 (0.0) c | 1.5 (1.0) ab | 1.8 (0.2) ab | 2.3 (0.9) a | 1.6 (0.7) ab | 0.9 (0.9) bc | 6.1 *** |
| Naphtalene | U7 | 7.6 (1.7) a | 3.9 (0.8) b | 3.5 (0.4) bc | 2.5 (1.0) c | 3.8 (0.4) bc | 3.6 (1.6) bc | 11.8 *** |
| 4,3 or2-Methyl-phenol | U9 | 3.4 (2.1) b | 7.0 (2.6) a | 8.1 (0.7) a | 7.5 (3.3) a | 6.5 (0.8) a | 6.2 (1.4) a | 4.9 ** |

578

579 Cast-A: fresh casts, known to be < 1 day; cast-B: fresh casts < 1 week old; cast-C: dry cast and probably more than 1 month old; cast-D: dry cast with marked signs of
580 degradation (greenish colour due to the presence algae with cracks at the surface), older than cast-C; cast-E: casts broken in small aggregates (10-13 mm) representing the last
581 state of degradation recognizable by naked eyes.

582 **Table 3:** Average values and standard deviation (n = 5) of Rock-Eval 6 thermal stability parameters for the five cast ageing stages and for
583 control aggregates (Ctrl) presenting no recent earthworm activity. Different letters indicate are statistically significant differences. (*** p <
584 0.001; ** p < 0.01; * p < 0.05 and ns for p > 0.05).

| Properties | Ctrl | Cast-A | Cast-B | Cast-C | Cast-D | Cast-E | F and p-values |
|---|---|---|---|---|---|---|---|
| HI (mg HC·$g^{-1}$ OC) | 154 (8) d | 185 (5) ab | 179 (6) bc | 190 (12) a | 176 (8) bc | 169 (13) c | 12.1*** |
| $OI_{RE6}$ (mg $O_2$·$g^{-1}$ OC) | 375 (47) a | 236 (15) cd | 241(10) cd | 229 (4) d | 2589 (9) bc | 284 (30) b | 30.1 *** |
| I-index | 0.07 (0.03) a | 0.08 (0.01) a | 0.07 (0.01) a | 0.08 (0.02) a | 0.08 (0.01) a | 0.04 (0.01) b | 2.8* |
| R-index | 0.62 (0.02) a | 0.61 (0.01) b | 0.61 (0.01) b | 0.60 (0.01) b | 0.61 (0.01) b | 0.63 (0.01) a | 4.3** |
| $T_{50\_CO2\_PYR}$ | 402 (1) a | 398 (2) bc | 399 (1) bc | 396 (4) c | 400 (1) ab | 400 (1) ab | 4.9 ** |
| $T_{50\_CO2\_OX}$ | 395 (4) a | 382 (2) c | 386 (2) b | 387 (4) b | 386 (2) b | 388 (2) b | 11.6 *** |

585
586 Cast-A: fresh casts, known to be < 1 day; cast-B: fresh casts < 1 week old; cast-C: dry cast and probably more than 1 month old; cast-D: dry cast with marked signs of
587 degradation (greenish colour due to the presence algae with cracks at the surface), older than cast-C; cast-E: casts broken in small aggregates (10-13 mm) representing the last
588 state of degradation recognizable by naked eyes.
589

590

591

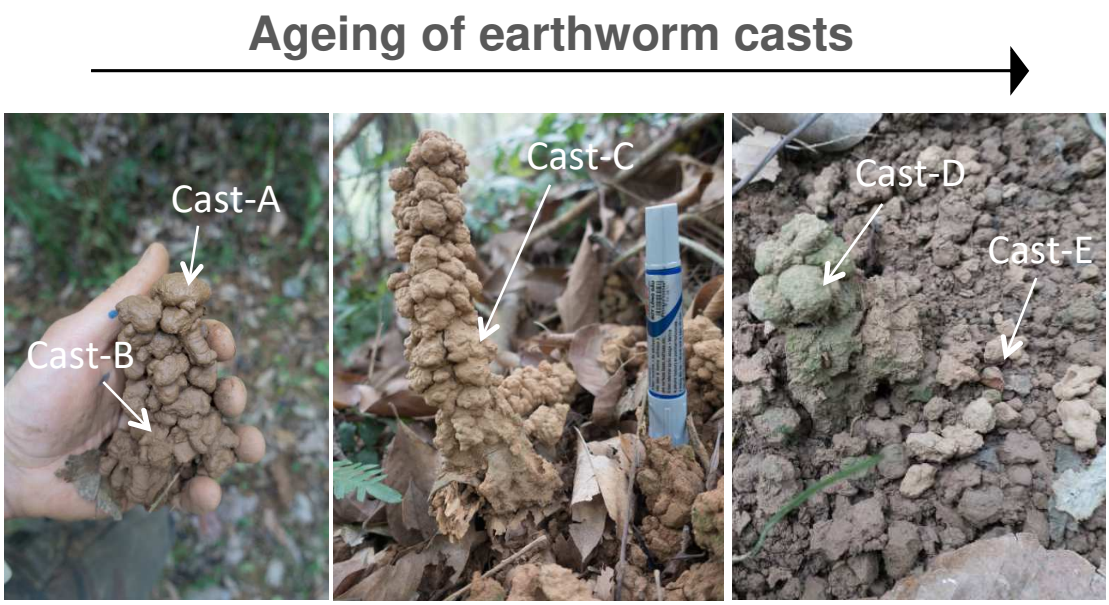


592

593 **Figure 1:** Earthworm cast ageing stages. Cast-A: fresh casts, known to be < 1 day;
594 cast-B: fresh casts < 1 week old; cast-C: dry cast and probably more than 1 month old;
595 cast-D: dry cast with marked signs of degradation (greenish colour due to the
596 presence algae with cracks at the surface), older than cast-C; cast-E: casts broken in
597 small aggregates (10-13 mm) representing the last state of degradation recognizable
598 by naked eyes possibly older than 1 year.

599

600

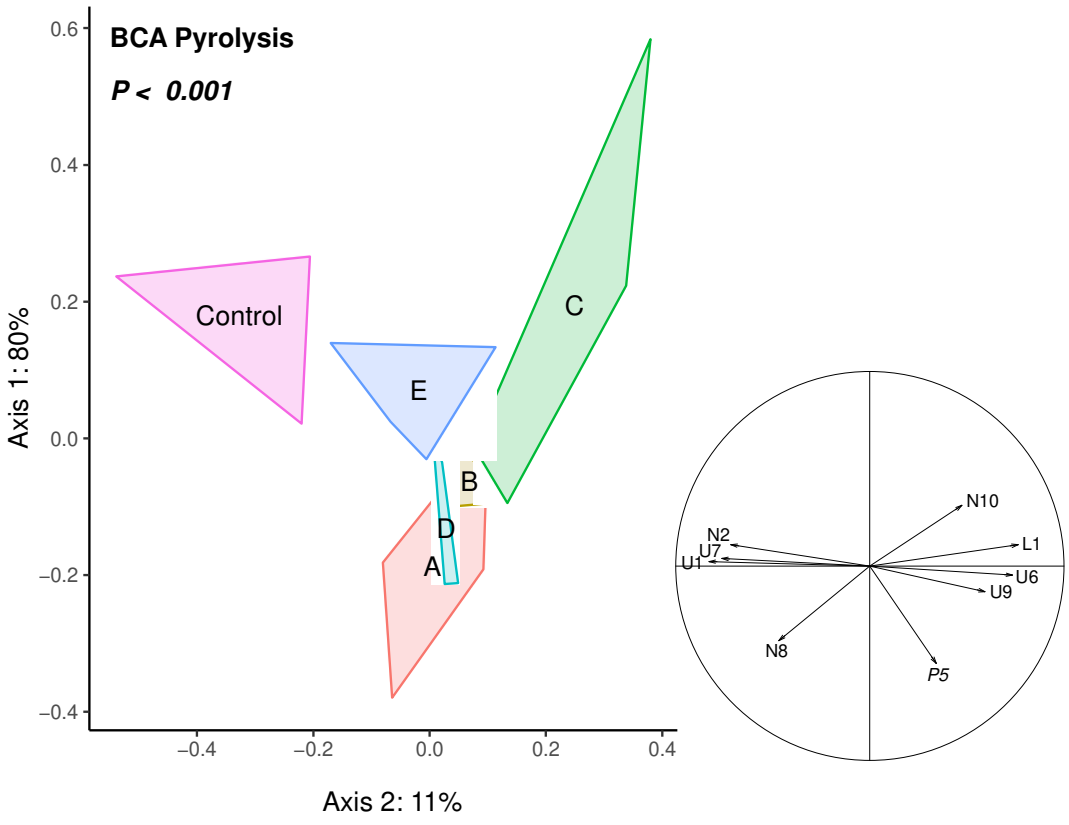


Cast-A: fresh casts, known to be < 1 day; cast-B: fresh casts < 1 week old; cast-C: dry cast and probably more than 1 month old; cast-D: dry cast with marked signs of degradation (greenish colour due to the presence algae with cracks at the surface), older than cast-C; cast-E: casts broken in small aggregates (10-13 mm) representing the last state of degradation recognizable by naked eyes.

**Figure 2:** Biplot showing the between components analysis (BCA) from variables describing the chemical composition OM for for the five cast ageing stages and for control aggregates (Ctrl) presenting no recent earthworm activity. Only significant compounds (Table 2) were included into the analysis. Variables are L1: 2-Methoxy-phenol (guaiacol), N2: Pyridine, N8: Benzonitrile, N10: Benzenepropanenitrile, U1: Benzene, U6: Acetic acid, U7: Naphtalene, U9: 4-Methyl-phenol/2- oder 3-Methyl-phenol.

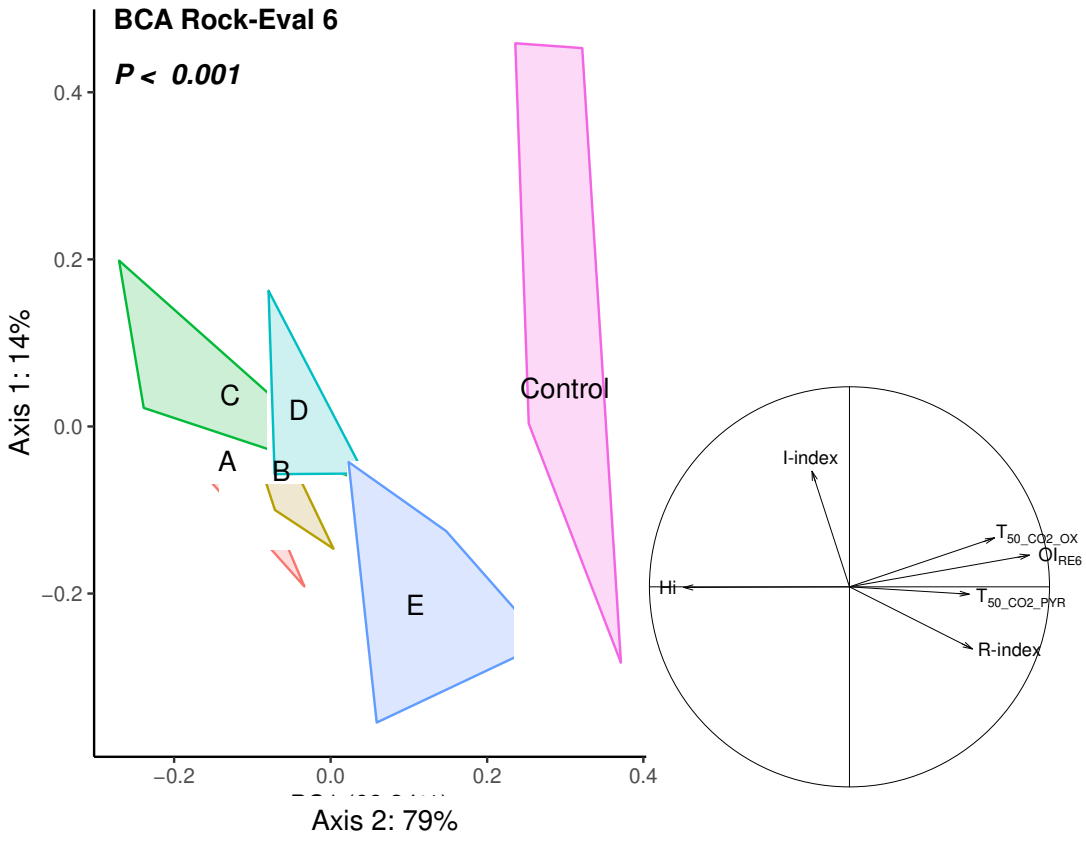


Cast-A: fresh casts, known to be < 1 day; cast-B: fresh casts < 1 week old; cast-C: dry cast and probably more than 1 month old; cast-D: dry cast with marked signs of degradation (greenish colour due to the presence algae with cracks at the surface), older than cast-C; cast-E: casts broken in small aggregates (10-13 mm) representing the last state of degradation recognizable by naked eyes.

**Figure 3:** Biplot showing the between components analysis (BCA) from variables describing the Rock-Eval 6 thermal stability parameters for the five cast ageing stages and for control aggregates (Ctrl) presenting no recent earthworm activity. Variables are hydrogen index (HI), oxygen index ($OI_{RE6}$), refractory index (R-index), immature index (I-index), and the temperature at which 50% of the $CO_2$ resulting from organic matter pyrolysis had evolved during pyrolysis and oxidation ($T_{50\_CO2\_PYR}$ and $T_{50\_CO2\_OX}$).

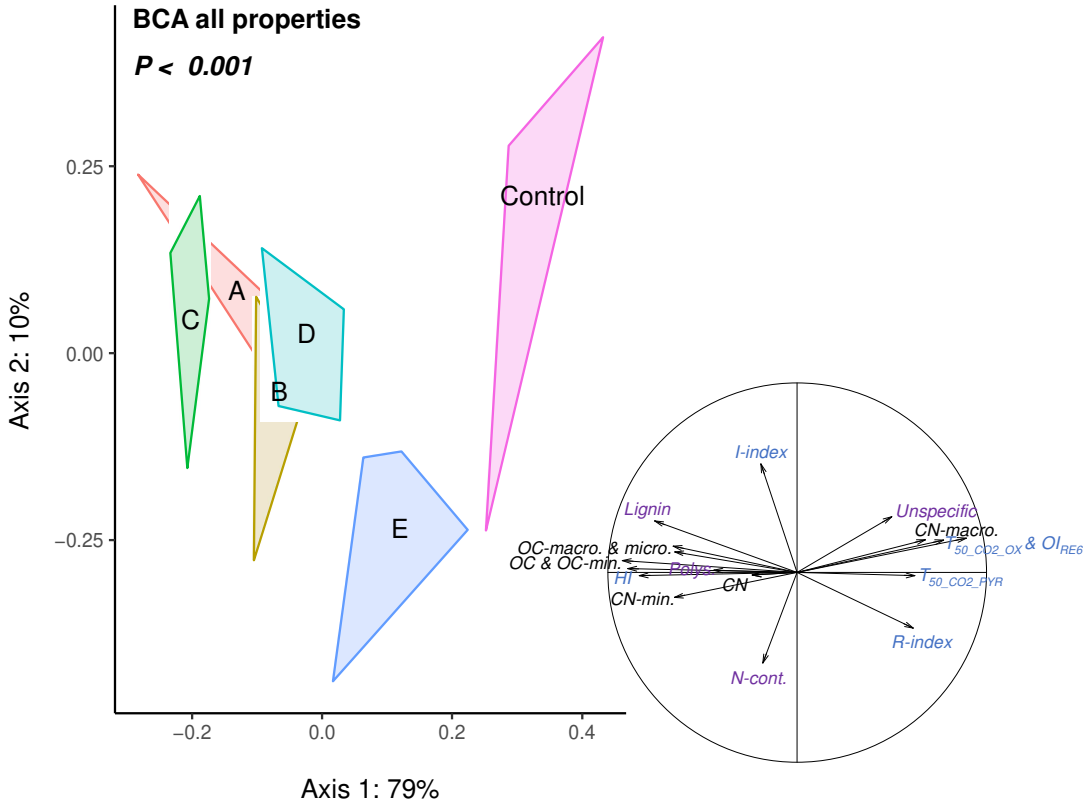


628

629 Cast-A: fresh casts, known to be < 1 day; cast-B: fresh casts < 1 week old; cast-C: dry cast and
630 probably more than 1 month old; cast-D: dry cast with marked signs of degradation (greenish colour
631 due to the presence algae with cracks at the surface), older than cast-C; cast-E: casts broken in small
632 aggregates (10-13 mm) representing the last state of degradation recognizable by naked eyes.
633

634 **Figure 4:** Biplot showing the between components analysis (BCA) from variables
635 describing OM for for the five cast ageing stages and for control aggregates (Ctrl)
636 presenting no recent earthworm activity. Variables in purple describe the OM
637 composition (lignin, N-containing, polysaccharides and unspecific), those in blue the
638 Rock-Eval 6 thermal stability parameters and those in black the OC content and C/N
639 ratio of the whole aggregate and the three physical fractions (macro-aggregate
640 (macro), micro-aggregates (micro) and mineral-associated (min)).
641

**Supplementary material**

**Table S1:** Average values (n = 5) for the five cast ageing stages and for control aggregates (Ctrl) presenting no recent earthworm activity. cast-A: fresh casts, assumed to be < 1 day and cast-B < 1 week old; cast-C: dry cast with a rounded shape and assumed to be more than 1 month old; cast-D: dry cast with visible signs of degradation (greenish colour with cracks at the surface); cast-E: broken casts in small aggregates representing the last state of degradation. Values bearing different letters are statistically significantly different. The numbers of stars for the significance level indicated the p-value range (*** $p < 0.001$; ** $p < 0.01$; * $p < 0.05$ and ns for $p > 0.05$).

| Origin | Code | Cast-A | Cast-B | Cast-C | Cast-D | Cast-E | Ctrl | F and p-values |
|---|---|---|---|---|---|---|---|---|
| Lignin (%) | L | 1.8 b | 0.8 c | 1.8 a | 0.5 c | 0.2 d | 0.0 d | 28.6 *** |
| 2-Methoxy-phenol (guaiacol) | L1 | 0.4 bc | 0.5 b | 0.9 a | 0.5 b | 0.2 cd | 0 d | 11.8*** |
| 2-Methoxy-4-(1-propenyl)-phenol (isoeugenol) | L2 | 0.3 | 0.3 | 0.9 | 0.0 | 0.0 | 0.0 | 1.8 ns |
| 1-(4-Hydroxy-3-methoxyphenyl)-ethanone | L3 | 1.1 | 0.0 | 0.0 | 0.0 | 0.0 | 0.0 | 1.6 ns |
| N-containing (%) | N | 33.4 | 37.1 | 36.2 | 33.6 | 38.6 | 31.9 | 2.3 ns |
| 1_Methyl-1H-pyrrole | N1 | 1.6 | 1.5 | 1.9 | 1.9 | 5.2 | 2.0 | 0.9 ns |
| Pyridine | N2 | 4.5 bc | 4.5 bc | 4.3 c | 5.3 b | 5.1 bc | 6.5 a | 6.9 *** |
| 2-Methyl-pyridine | N3 | 1.4 | 1.2 | 1.6 | 1.7 | 1.6 | 1.7 | 1.9 ns |
| 3-Methyl-pyridine | N4 | 2.1 | 2.1 | 4.6 | 2.4 | 2.5 | 2.5 | 1.8 ns |
| 1H-Pyrrole /Pyrrole | N5 | 2.3 | 2.0 | 2.5 | 2.5 | 1.7 | 2.0 | 1.5 ns |
| 3-Methyl-1H-pyrrole /2-Methyl-1H-pyrrole | N6 | 1.2 | 1.1 | 2.2 | 1.3 | 1.9 | 1.1 | 1.9 ns |
| 3-Methyl-1H-pyrrole | N7 | 1.4 | 1.2 | 1.4 | 1.4 | 2.0 | 1.0 | 1.5 ns |
| Benzonitrile | N8 | 4.8 ab | 3.6 abc | 2.6 c | 4.0 ab | 3.3 bc | 4.8 a | 3.1 * |
| Benzeneacetronitrile | N9 | 0.6 | 2.2 | 0.0 | 0.0 | 0.0 | 0.0 | 0.9 ns |

| | | | | | | | | |
|---|---|---|---|---|---|---|---|---|
| Benzenepropanenitrile | N10 | 0.9 b | 0.8 b | 2.4 a | 0.9 b | 0.8 b | 0.3 b | 2.9 * |
| 1H-Indole /Indole | N11 | 6.2 | 8.5 | 6.1 | 5.4 | 6.0 | 4.3 | 2.2 ns |
| 3-Methyl-1H-indole | N12 | 6.6 | 8.5 | 6.6 | 6.9 | 8.4 | 5.7 | 1.1 ns |
| Polysaccharides (%) | P | 14.5 | 12.6 | 16.6 | 16.4 | 13.5 | 10.8 | 2.4 ns |
| 2-Methyl-Furan | P1 | 1.9 | 1.8 | 4.3 | 2.3 | 2.5 | 2.3 | 1.1 ns |
| 1-Heptyl-2-methyl-cyclopropane | P2 | 0.5 | 0.3 | 0.4 | 0.4 | 0.9 | 0.1 | 1.2 ns |
| 2-Cyclopentene-1-one | P3 | 3.5 | 3.0 | 2.4 | 3.5 | 2.7 | 2.5 | 1.6 ns |
| 2-Methyl-2-cyclopentene-1-one | P4 | 1.7 | 1.6 | 2.7 | 2.2 | 1.9 | 1.9 | 0.7 ns |
| Furfural | P5 | 3.4 ab | 2.8 abc | 2.4 bc | 3.9 a | 2.0 bc | 1.5 c | 3.4 * |
| 3-Methyl-2-cyclopentene-1-one | P6 | 1.8 | 1.5 | 1.8 | 2.0 | 1.6 | 1.3 | 1.6 ns |
| 2,3-Dimethyl-cyclopenten-1-one | P7 | 0.8 | 0.7 | 1.4 | 0.9 | 1.0 | 0.7 | 2.4 ns |
| 5-Methyl-2-furancarboxaldehyde | P8 | 1.0 | 0.8 | 1.3 | 1.3 | 0.9 | 0.5 | 1.6 ns |
| Unspecific (%) | U | 50.3 b | 49.6 b | 45.4 b | 49.5 b | 47.7 b | 57.2 a | 2.9 * |
| Benzene | U1 | 8.8 b | 7.8 b | 5.5 b | 8.1 b | 8.1 b | 17.1 a | 8.1 *** |
| Toluene | U2 | 9.4 | 7.8 | 8.5 | 9.0 | 7.2 | 9.6 | 0.9 ns |
| Ethylbenzene | U3 | 1.5 | 1.3 | 1.6 | 1.5 | 1.4 | 1.4 | 0.6 ns |
| 1,3-Dimethyl-benzene | U4 | 1.2 | 1.1 | 2.9 | 1.3 | 4.6 | 1.1 | 0.9 ns |
| Styrene | U5 | 2.2 | 1.7 | 1.6 | 2.1 | 1.8 | 2.4 | 2.4 ns |
| Acetic acid | U6 | 1.5 ab | 1.8 ab | 2.3 a | 1.6 ab | 0.9 bc | 0.0 c | 6.1 *** |
| Naphtalene | U7 | 3.9 b | 3.5 bc | 2.5 c | 3.8 bc | 3.6 bc | 7.6 a | 11.8 *** |
| Phenol | U8 | 8.7 | 8.5 | 7.0 | 9.4 | 8.0 | 9.0 | 0.3 ns |
| 4-Methyl-phenol/2- oder 3-Methyl-phenol | U9 | 7.0 a | 8.1 a | 7.5 a | 6.5 a | 6.2 a | 3.4 b | 4.9 ** |
| 3-Ethyl-phenol | U10 | 1.7 | 2.4 | 1.9 | 2.2 | 1.9 | 1.2 | 2.6 ns |
| Fluorene | U11 | 4.5 | 5.7 | 4.1 | 4.0 | 4.0 | 4.6 | 0.8 ns |

648

Cast ageing stages

A

B

C

D

E

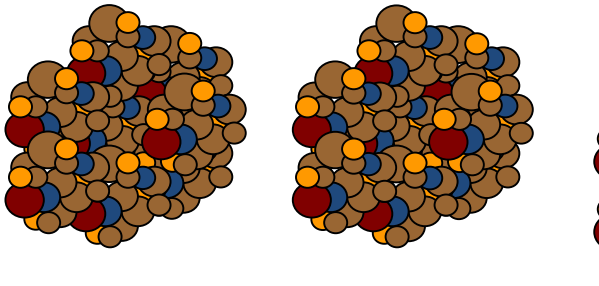

***Anecic species***

**Stress**
(rainfall, animal trampling….)

oPOM

Microagg

MOM